

The power of negative thinking

Liang Zhan^{1*}, Lisanne M. Jenkins², Ouri E. Wolfson³, Johnson J. GadElkarim⁴,
Paul M. Thompson⁵, Olusola A. Ajilore², Moo K. Chung⁶, Alex D. Leow^{2, 4*}

¹Computer Engineering Program, University of Wisconsin-Stout, Menomonie, WI, USA

²Department of Psychiatry, University of Illinois, Chicago, IL, USA

³Department of Computer Science, University of Illinois, Chicago, IL, USA

⁴Department of Bioengineering, University of Illinois, Chicago, IL, USA

⁵Imaging Genetics Center, and Institute for Neuroimaging and Informatics, Keck School of
Medicine of USC, CA, USA

⁶Department of Biostatistics and Medical Informatics, University of Wisconsin-Madison, Madison,
WI, USA

* Leow and Zhan share corresponding author

Alex Leow, Departments of Psychiatry and Bioengineering, The University of
Illinois at Chicago, 1601 W Taylor St, M/C 912, Chicago, IL, 60612, USA. Email:
Email: aleow@psych.uic.edu.

Liang Zhan, Computer Engineering Program, University of Wisconsin-Stout, 329
Fryklund Hall, 807 3rd Street E., Menomonie, WI 54751, USA

Email: zhanl@uwstout.edu

Word count: 3668

Abstract

Heuristically adapted from methods originally developed for social networks, current network modularity approaches to account for negative BOLD-signal correlations in fMRI-derived connectomes yield variable results with suboptimal reproducibility. As an alternative, we propose a new, reproducible approach that exploits how frequent the BOLD-signal correlation between two nodes is negative. We validated this novel probability-based modularity approach on two independent publically available resting state connectome datasets (the Human Connectome Project and the 1000 Functional Connectomes) and demonstrated that negative correlations alone are sufficient in understanding resting-state fMRI connectome modularity. In fact, this approach permits a dual formulation that leads to equivalent solutions regardless of whether one considers positive or negative edges. Results confirmed the superiority of our approach in that: 1) correlations with highest probability of being negative are consistently placed between modules, 2) due to the equivalent dual forms, no arbitrary weighting factor is required to balance the influence between negative and positive correlations, as is currently employed in all Q modularity-based approaches.

Introduction

Just as social networks can be divided into cliques that describe modes of association (e.g. family, school), the brain's connectome can be divided into modules or communities. Modules contain a series of nodes that are densely interconnected (via edges) with one another but weakly connected with nodes in other modules (Meunier, Lambiotte, & Bullmore, 2010). Thus modularity or community structure best describes the intermediate scale of network organization, rather than the global or local scale. In many networks, modules can be divided into smaller sub-modules, thus can be said to demonstrate hierarchical modularity or *near decomposability*, a term first coined by Simon in 1962 (Meunier et al., 2010; Simon, 2002). Modules in fMRI-derived networks tend to comprise anatomically and/or functionally related regions, and the presence of modularity in a network has several advantages, including greater adaptability and robustness of the function of the network. Understanding modularity of brain networks can inform the study of organization and mechanisms of brain function and dysfunction, thus potentially the treatment of neuropsychiatric diseases.

Mathematical techniques derived from graph theory (Fornito, Zalesky, & Breakspear, 2013) have been developed to measure and describe the modular organization of neural connectomes (Bullmore & Sporns, 2009; Sporns & Betzel, 2016). Different methods for module detection have been applied in network neuroscience, and offer different strengths and weaknesses (reviewed in Sporns & Betzel, 2016). Optimization algorithms are typically used to maximize modular

structure Q , rather than calculate it directly (Danon, Diaz-Guilera, Duch, & Arenas, 2005). These algorithms vary in accuracy as there are tradeoffs made with computational speed (Rubinov and Sporns, 2010). Simulated annealing (e.g. Guimera & Amaral, 2005; Guimera, Sales-Pardo, & Amaral, 2004) is a slower, more accurate method for smaller networks, however could take several months of continuous computations with larger networks (Danon et al., 2005). The Newman method (2006; Newman & Girvan, 2004) reformulates modularity with consideration of the spectral properties of the network, and is also considered fairly accurate with adequate speed for smaller networks (Rubinov and Sporns, 2010). More recently, the Louvain method (Blondel, Guillaume, Lambiotte, & Lefebvre, 2008) has been developed for large networks (millions of nodes and billions of edges). Its rapid computation and ability to detect modular hierarchy (Rubinov & Sporns, 2010) has led to it becoming one of the most widely utilized methods for detecting communities in large networks. Comparisons with other modularity optimization methods have found that the Louvain method outperforms numerous other similar methods (Aynaoud, Blondel, Guillaume, & Lambiotte, 2013; Lancichinetti & Fortunato, 2009).

These earlier methods originally developed out of social sciences (e.g. for social network analysis) and are problematic as they lack reproducibility, often failing replication (Butts, 2003; Fortunato & Barthelemy, 2007; Guimera & Sales-Pardo, 2009). With the advent of connectomics, they also have been heuristically applied to fMRI brain networks, however these networks have the additional complication of negative correlations. To this end, early methods largely ignore

fMRI networks' negative edges (Fornito et al., 2013), only considering the right tail of the correlation histogram, i.e. the positive edges (Schwarz & McGonigle, 2011). However, in functional neuroimaging, negative edges may be neurobiologically relevant (Sporns & Betzel, 2016), depending on factors such as data preprocessing steps, particularly the removal of potentially confounding signal such as head motion, global white-matter or whole-brain average signal, before calculation of the correlation matrix, because removal of such signal could result in detection of anticorrelations that were not present in the original data (Schwarz & McGonigle, 2011). Ignoring negative edges is achieved with binarization of a network (so-called 'hard thresholding'), by selecting a threshold then replacing edge values below this threshold with zeros, and replacing supra-threshold values with ones. Some researchers retain the weights of the supra-threshold edge values, which has the effect of compressing the positive edges, however the negative edges remain suppressed (Schwarz & McGonigle, 2011). Choice of threshold is important as more severe thresholds increase the contributions from the strongest edges, but can result in excessive disconnection of nodes within networks, in comparison to less stringent thresholds. Rather than binarizing networks, some researchers choose a 'soft thresholding' approach that replaces thresholding with a continuous mapping of correlation values into edge weights, which had the effect of suppressing, rather than removing weaker connections (Schwarz & McGonigle, 2011). Linear and non-linear adjacency functions can be employed, and the choice can be made to retain the valence of the edge weights, when appropriate.

An alternative to optimization methods discussed above, Independent Components Analysis (ICA) has been applied to functional neuroimaging data (Beckmann, DeLuca, Devlin, & Smith, 2005). This method assumes that voxel time series are linear combinations of subsets of representative time series (Sporns & Betzel, 2016). Patterns of voxels load onto spatially independent components (modules). Unlike optimization methods, ICA allows for overlapping communities (Sporns & Betzel, 2016), although the number of ICA components needs to be pre-specified.

Utilizing a distance-based approach, recently, a new technique for investigating the hierarchical modularity of structural brain networks has been developed (GadElkarim et al., 2014; GadElkarim et al., 2012). Rather than using Q or detecting spatially independent components, Path Length Associated Community Estimation (PLACE) uses a unique metric Ψ^{PL} . This metric measures the difference in path length between versus within modules, to both maximize within-module integration and between-module separation (GadElkarim et al., 2014). It utilizes a hierarchically iterative procedure to compute global-to-local bifurcating trees (i.e. dendrograms), each of which represents a collection of nodes that form a module.

In this study we demonstrate a related method for functional brain networks – Probability Associated Community Estimation (PACE), that uses probability, not thresholds or the magnitude of BOLD signal correlations. We compare this method to five different implementations within the widely used Brain Connectivity Toolbox (BCT) (<http://www.brain-connectivity-toolbox.net/>).

We used data from the freely accessible 1000 Functional Connectomes or F1000 Project dataset (Biswal et al., 2010) and the Human Connectome Project (HCP) (Van Essen et al., 2013; Van Essen et al., 2012) to validate this method, and to examine differences in resting-state functional connectome's modularity (i.e., the resting-state networks or RSN) between males and females.

(online) Methods

The popular Q-based modular structure (Blondel et al., 2008; Reichardt & Bornholdt, 2006; Ronhovde & Nussinov, 2009; Rubinov & Sporns, 2011; Sun, Danila, Josic, & Bassler, 2009) is extracted by finding the set of non-overlapping modules that maximizes the modularity Q (or weighted modularity metric Q_w):

$$Q(G) = \frac{1}{2m} \sum_{i \neq j} \left(A_{ij} - \frac{k_i k_j}{2m} \right) \delta(i, j)$$

Adapted from social network sciences, these Q-based approaches are naturally suitable for understanding the modularity of structural connectome where all edges are non-negative. As an alternative to Q, we previously developed a graph distance (shortest path length) based modularity approach for the structural connectome. By exploiting the structural connectome's *hierarchical modularity*, this *path length associated community estimation technique* (PLACE) is designed to extract global-to-local hierarchical modular structure in the form of bifurcating dendrograms (GadElkarim et al., 2012). PLACE has potential advantages over Q (GadElkarim et al., 2014), as it is hierarchically regular and thus *scalable* by design. Here, the degree to which nodes are separated is measured using graph distances (Dijkstra, 1959) and the PLACE benefit function is the Ψ^{PL} metric, defined at each bifurcation as the difference between the mean inter- and intra-modular graph distances. Thus, maximizing Ψ^{PL} is equivalent to searching for a partition with stronger intra-community integration and stronger between-community separation.

Probability-associated community estimation (PACE) for functional connectomes

Here let us describe the PACE-based modularity of a functional connectome mathematically represented as an undirected graph $FC(V, E)$, where V is a set of vertices (i.e., nodes) and E is a set of edges (indexed by considering all pairs of vertices). Each edge of E is associated with a weight that can be either positive or negative.

Given a collection of functional connectomes S on the same set of nodes V (but having edges with different weights), we can define the following *aggregation graph* $G(V, E)$. For each edge $e_{i,j}$ in E connecting node i and node j , we consider $P^-_{i,j}$, the probability of observing a negative value at this edge in S (i.e., the BOLD signals of i and j are anti-correlated). In the case of HCP, for example, S thus consists of all healthy subjects' resting-state functional connectome and this probability can be estimated using the ratio between the number of connectomes in S having the edge $e_{i,j} < 0$ and the total number of connectomes in S . Similarly, we define the probability of an edge in E being non-negative as $P^+_{i,j}$. Naturally, the $P^- - P^+$ pair satisfies the following relationship:

$$P^-_{i,j} + P^+_{i,j} = 1, \quad \forall (i,j), i \neq j$$

Then, inspired by PLACE, given C^1, C^2, \dots, C^N that are N subsets (or communities) of V , we define the mean intra-community edge positivity or negativity $\overline{P^\pm(C^n)}$ for the n -th community C^n as:

$$\overline{P^\pm(C^n)} = \frac{\sum_{i,j \in C^n, i < j} P^\pm_{i,j}}{|C^n|(|C^n| - 1)/2}$$

Here $|C^n|$ represents the size (i.e., number of nodes) of the n -th community. Similarly, we could define the mean inter-community edge positivity and negativity (between communities C^n and C^m) as:

$$\overline{P^\pm(C^n, C^m)} = \overline{P^\pm(C^m, C^n)} = \frac{\sum_{i \in C^n, j \in C^m} P^\pm_{i,j}}{|C^n||C^m|}$$

Here, the first equality holds as correlation-based functional connectomes are undirected. The intuition of PACE for fMRI connectomes is that edges that are most frequently anti-correlations should be placed across communities.

PACE operates as follows. Given a collection of functional connectomes S , PACE identifies a natural number N and a partition of V , $C^1 \cup C^2 \cup \dots \cup C^N = V$, ($C^i \cap C^j = \emptyset$ for all $i \neq j$) which maximizes the PACE benefit function Ψ^P . Intuitively, Ψ^P computes the difference between mean inter-community edge negativity and mean intra-community edge negativity. Moreover, considering the duality between P^- and P^+ , our optimization problem thus permits an equivalent dual form. Formally, $\Psi^P =$

$$\operatorname{argmax}_{C^1 \cup C^2 \cup \dots \cup C^N = V, C^i \cap C^j = \emptyset \text{ for all } i \neq j} \left\{ \frac{\sum_{1 \leq n < m \leq N} \overline{P^-(C^n, C^m)}}{N(N-1)/2} - \frac{\sum_{1 \leq n \leq N} \overline{P^-(C^n)}}{N} \right\} =$$

$$\operatorname{argmax}_{C^1 \cup C^2 \cup \dots \cup C^N = V, C^i \cap C^j = \emptyset \text{ for all } i \neq j} \left\{ \frac{\sum_{1 \leq n \leq N} \overline{P^+(C^n)}}{N} - \frac{\sum_{1 \leq n < m \leq N} \overline{P^+(C^n, C^m)}}{N(N-1)/2} \right\}$$

To solve the above NP-hard PACE optimization problem that captures the hierarchical configuration of the functional connectome (Meunier et al., 2010), we

adopt a PLACE-like algorithm, which has been extensively validated (Ajilore et al., 2013; GadElkarim et al., 2014; GadElkarim et al., 2012; Lamar et al., 2016; Ye et al., 2015; Zhang et al., 2016), and computed global-to-local 4-level bifurcating trees (yielding a total of 16 communities at the fourth level; please refer to GadElkarim et al. (2014) for implementation details).

Results

Data description

We tested our PACE framework on two publically available connectome datasets (Biswal et al., 2010; Brown, Rudie, Bandrowski, Van Horn, & Bookheimer, 2012). The first one is a 986-subject resting state fMRI connectome dataset from the 1000 functional connectome project (17 subjects' connectomes were discarded due to corrupted files), downloaded from the USC multimodal connectivity database (<http://umcd.humanconnectomeproject.org>). The dimension of the network is 177x177. The 2nd dataset is 820 subjects' resting state fMRI connectome from the Human Connectome Project (released in December 2015, named as HCP900 Parcellation+Timeseries+Netmats, https://db.humanconnectome.org/data/projects/HCP_900). The dimension of the network is 200x200, derived using ICA. For details of these two datasets, please refer to relevant information on their respective websites and related references.

Table 1 Summarizes the six Q-based methods, as implemented in the BCT toolbox, tested and compared in this study (Betzel, Fukushima, He, Zuo, & Sporns, 2016; Rubinov & Sporns, 2011; Schwarz & McGonigle, 2011).

Weighted version	Q-Comb-Sym	$Q = C^+Q^+ - C^-Q^-$ $C^+ = C^-$	$Q^+ = f(W_{ij}^+)$ $W_{ij}^+ = \begin{cases} W_{ij} & \text{if } W_{ij} > 0 \\ 0 & \text{otherwise} \end{cases}$	$Q^- = f(W_{ij}^-)$ $W_{ij}^- = \begin{cases} -W_{ij} & \text{if } W_{ij} < 0 \\ 0 & \text{otherwise} \end{cases}$
	Q-Comb-Asym	$Q = C^+Q^+ - C^-Q^-$ $C^+ \neq C^-$		
	Q-Positive-only	$Q = f(W_{ij}^+)$	$W_{ij}^+ = \begin{cases} W_{ij} & \text{if } W_{ij} > 0 \\ 0 & \text{otherwise} \end{cases}$	
	Q-Amplitude	$Q = f(W_{ij})$	$ W_{ij} = \begin{cases} W_{ij} & \text{if } W_{ij} > 0 \\ -W_{ij} & \text{otherwise} \end{cases}$	
	Q-Negative-only	$Q = f(W_{ij}^-)$	$W_{ij}^- = \begin{cases} -W_{ij} & \text{if } W_{ij} < 0 \\ 0 & \text{otherwise} \end{cases}$	
Binarizing	Thresholding	$Q = f(B_{ij})$	$B_{ij} = \begin{cases} 1 & \text{if } W_{ij} > \text{thres} \\ 0 & \text{otherwise} \end{cases}$	

Modular structures revealed using PACE versus Q-based weighted methods

We compared PACE with Q-based methods in the reproducibility and stability of the resulting modularity computed from the mean F1000 or HCP functional connectome (mean connectome is computed by element-wise averaging). **Table 1** lists six Q-based methods adopted in this study (five weighted and one binarized). We conducted 100 runs for each of the six methods as well as PACE, and quantified pairwise similarity between two modular structures using the normalized mutual information (NMI; Alexander-Bloch et al.,

2012). NMI values are between 0 and 1, with 1 indicating two modular structures are identical. We report summary statistics of these pairwise NMI values in **Table 2a** (the total number of NMI values are $4950=100 \times 99/2$). As shown in this table, Q-based methods produced substantially variable modular structures across runs (and the number of communities across runs is also variable). By contrast, PACE produced identical results up to the third level (i.e., 8 communities) for HCP and throughout all four levels for F1000.

To visualize these modularity results, we show axial slices of representative modular structures, for the HCP dataset, generated using different methods (**Figure 1**, also see **Figure 2a** for rearranged connectome matrices based on PACE).

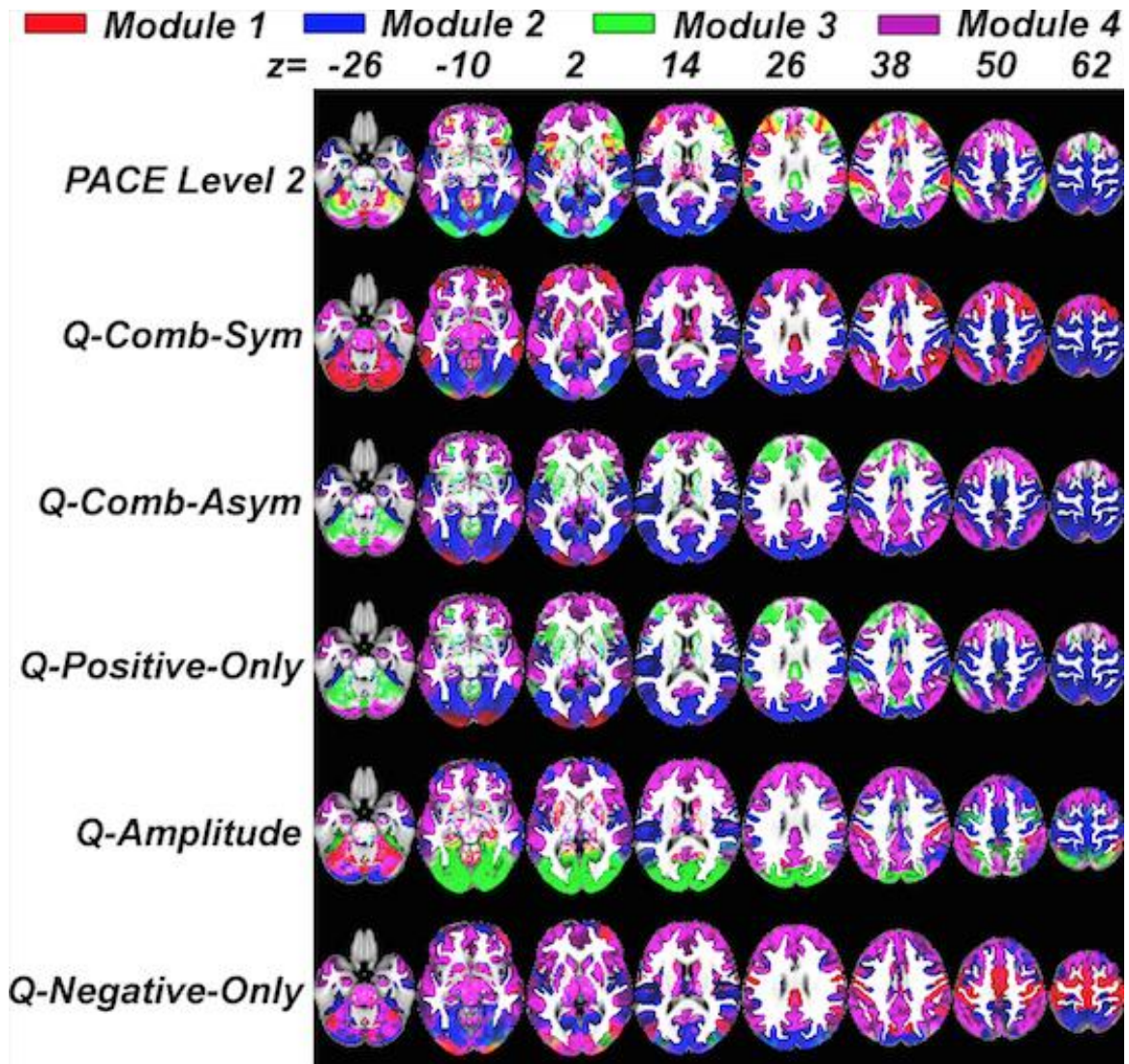


Figure 1. Representative modular structures generated using different methods for the HCP dataset. Regions coded in the same color (out of four: green, blue, red, and violet) form a distinct community or module. Note that unlike F1000, which uses structure parcellation to partition networks into non-overlapping communities, HCP utilizes an ICA-based parcellation, which allows components (modules) to overlap (Sporns & Betzel, 2016), resulting in regions with mixed colors (e.g. yellow).

As Q-based methods yielded variable results (with variable number of communities, see **Table 2a**), for a fair comparison we randomly select a four-community modular structure to visualize each of the five Q-based methods.

Visually, except for the Q-Amplitude and Q-negative-only, Q-based results shared similarities with results generated using 2nd-level PACE (variability among Q-based methods notwithstanding).

Table 2b summarizes, for each Q-based method, the mean and standard deviation of NMI between the 100 runs and 2nd-level PACE-derived modularity.

Table 2. (a). Mean and standard deviation of pair-wise Normalized Mutual Information (NMI) across 100 repeated runs within each method. For Q-based methods, the most reproducible methods are highlighted in bold (for F1000 it was the Q-Comb-Sym, and for HCP the Q-Positive-only). **(b).** For each Q-based method, this table summarizes the mean and standard deviation of pair-wise NMI between the repeated 100 runs and 2nd-level PACE-derived modularity.

2a				
	F1000		HCP	
	NMI	Number of Modules (Number of runs)	NMI	Number of Modules (Number of runs)
PACE Level 1	1.0±0.0	2(100)	1.0±0.0	2(100)
PACE Level 2	1.0±0.0	4(100)	1.0±0.0	4(100)
PACE Level 3	1.0±0.0	8(100)	1.0±0.0	8(100)
PACE Level 4	1.0±0.0	16(100)	0.9996±0.0016	16(100)
Q-Comb-Sym	0.896±0.093	3(97),4(3)	0.731±0.160	3(38), 4(62)
Q-Comb-Asym	0.835±0.091	3(63),4(37)	0.772±0.134	3(31),4(69)
Q-Positive-only	0.844±0.103	3(1),4(99)	0.834±0.079	3(41),4(59)
Q-Amplitude	0.819±0.108	4(18),5(74),6(8)	0.614±0.135	3(1),4(49),5(36),6(14)
Q-Negative-only	0.617±0.158	3(66),4(34)	0.460±0.129	3(3),4(61),5(36)

2b		
	F1000	HCP
Q-Comb-Sym	0.725±0.026	0.576±0.051
Q-Comb-Asym	0.705±0.043	0.603±0.047
Q-Positive-only	0.740±0.061	0.539±0.035
Q-Amplitude	0.606±0.064	0.235±0.027
Q-Negative-only	0.170±0.013	0.113±0.017

Lastly, to further appreciate the effect of variable numbers of modules in Q-based methods, we randomly selected and visualized one 3-community and one 4-community Q-derived HCP modular structure. This is displayed in **Figure 2b**, with the visualizations again demonstrating the problem of reproducibility with Q (for comparison, the 1st level 2-community and 2nd-level 4-community PACE HCP results are also shown).

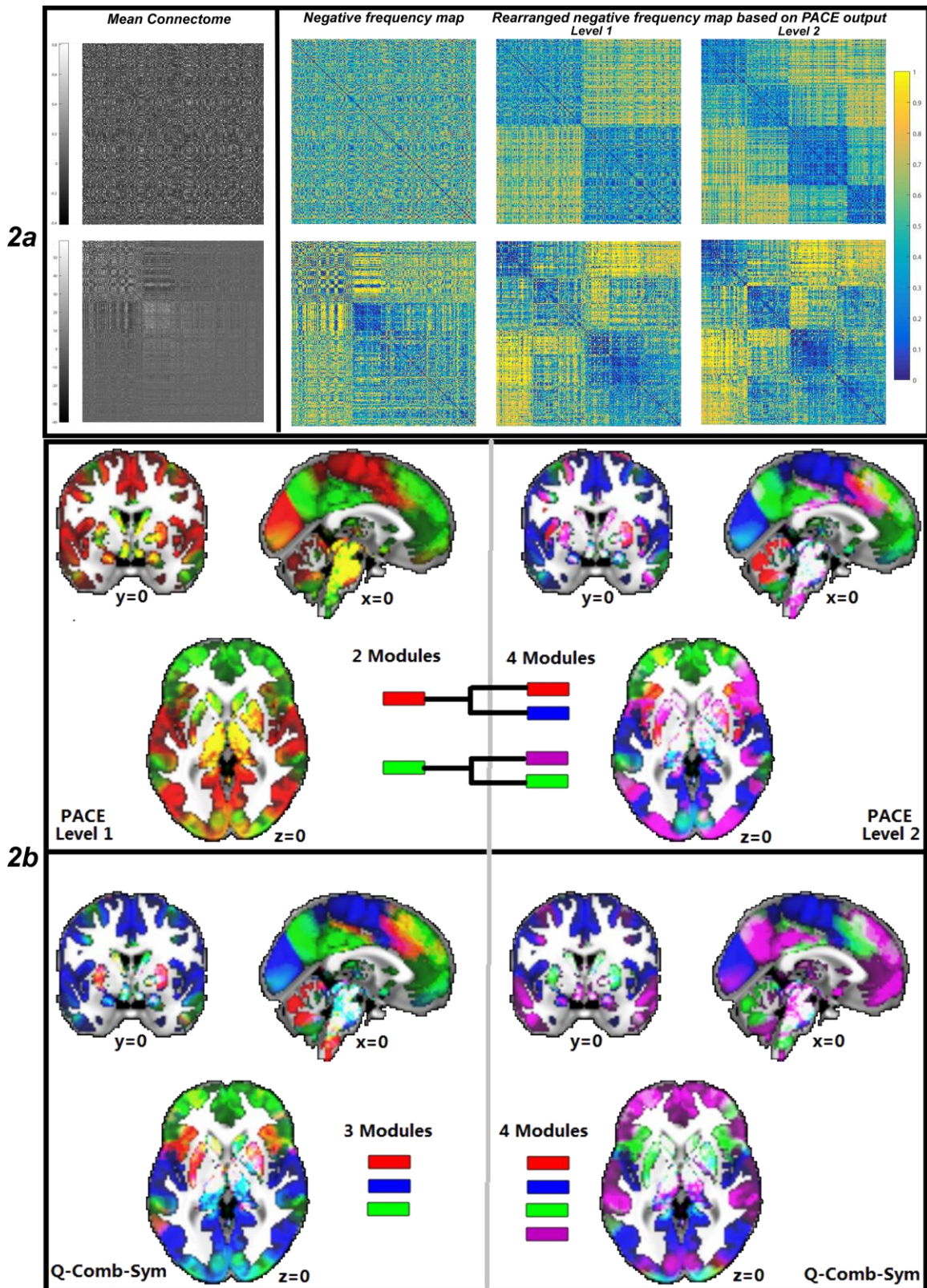


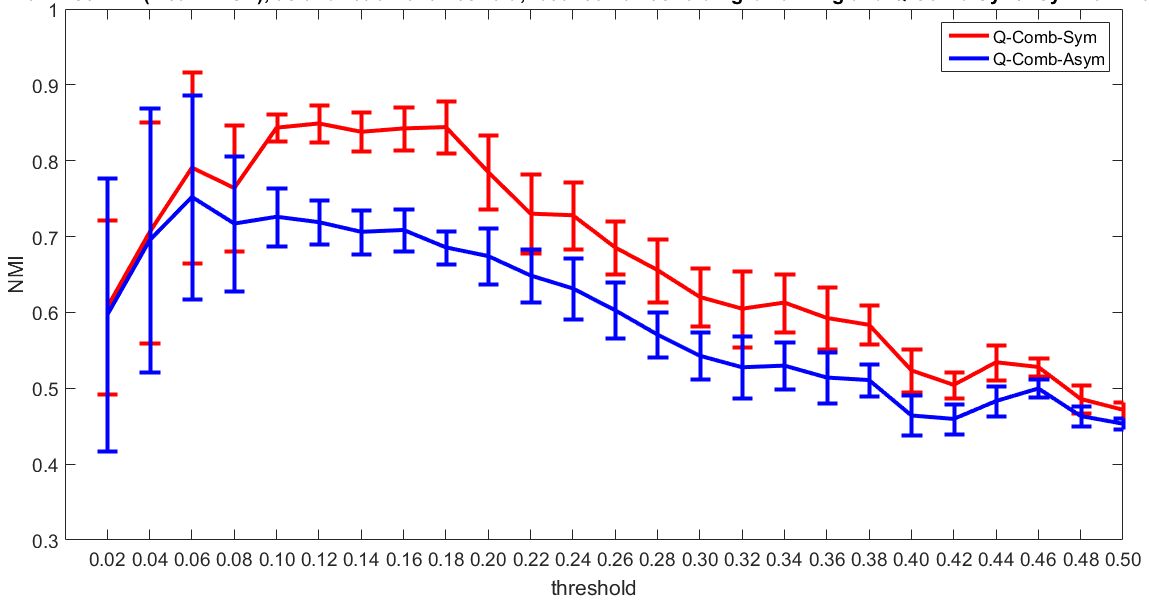
Figure 2 (a) shows, for the F1000 (first row) and the HCP (2nd row) dataset: 1) first column: the mean resting-state functional connectome matrices (mean is computed by

element-wise averaging); 2) second column: the negative frequency matrices; 3) third and fourth column: the rearranged matrices based on modularity extracted using Level 1 and Level 2 PACE. **(b)** visualizes randomly selected 3-community and 4-community Q-derived modular structures in HCP, demonstrating the problem of reproducibility with Q. For comparison, the 1st level 2-community and 2nd-level 4-community PACE results are also shown.

Variability in the modular structure computed using Q-based thresholding-binarizing method

For the sixth Q-based modularity method, which applies an arbitrary non-negative threshold to the mean connectome followed by binarization (all edges below threshold set to zero, and above threshold to one), we again conducted 100 runs for each threshold (starting, as a fraction of the maximum value in the mean functional connectome, from 0 to 0.5 with increments of 0.02) using the unweighted Louvain method routine implemented in the BCT toolbox. **Figure 3** plots the mean pairwise NMI \pm SD as a function of the threshold, between each of the 100 runs and those generated using the Q-Comb-Sym or Q-Comb-Asym methods. Results again demonstrated the high degree of variability, especially in the case of HCP.

Pairwise NMI (Mean \pm SD), as a function of threshold, between thresholding-binarizing and Q-Comb-Sym/Asym for F1000



Pairwise NMI (Mean \pm SD), as a function of threshold, between thresholding-binarizing and Q-Comb-Sym/Asym for HCP

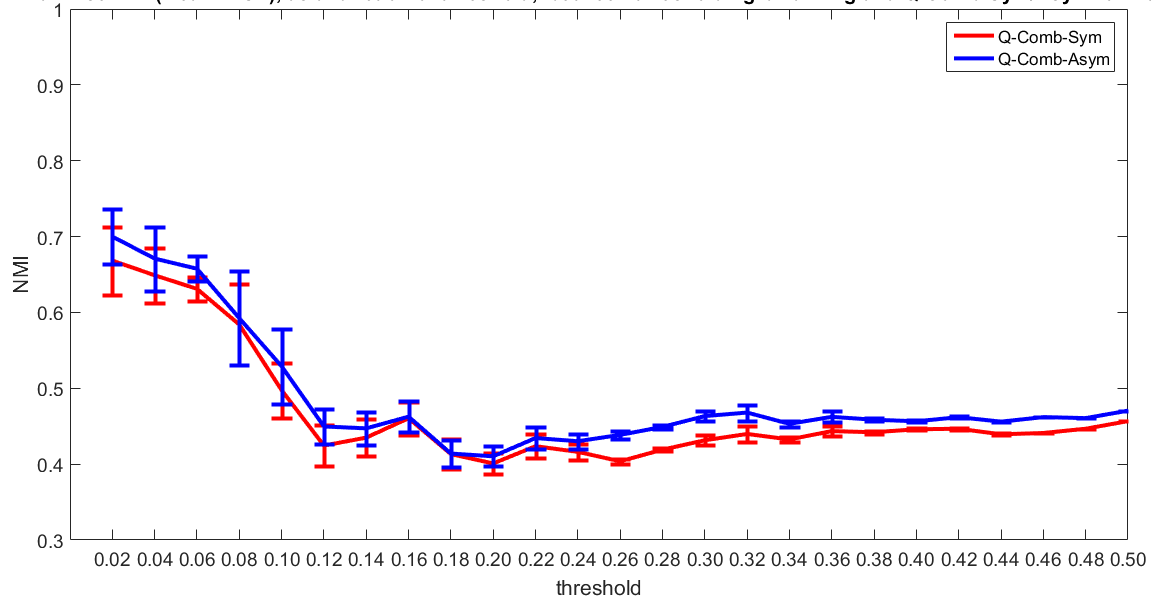


Figure 3. Mean and standard deviation of pair-wise similarity metric NMI, as a function of the threshold (x-axis, as a fraction of the maximal value in the mean group connectome), between the modularity extracted using Q-based thresholding-binarizing and the weighted Q-Comb-Sym method or the Q-Comb-Asym method for F1000 (top) and HCP (bottom).

Sex differences in resting-state networks using a PACE-based hierarchical permutation procedure

Because the HCP dataset contains subjects with the narrow age range of 22-35 (Van Essen et al., 2013; Van Essen et al., 2012), we demonstrate here that the stability of PACE makes it possible to pinpoint modularity differences between males and females in the HCP dataset, whilst minimizing potential confounding influences of age. As PACE uses a hierarchical permutation procedure to create trees, controlling for multiple comparisons is straightforward. Here, if two modular structures exhibit significant differences at each of the m most-local levels of modular hierarchy (each of them controlled at 0.05), collectively it would yield a combined false positive rate of 0.05 to the power of m . For the actual permutation procedure, we first computed the NMI between the two PACE-derived modular structures generated from the 367 males and the 453 females in the HCP dataset. Then, under the null hypothesis (no sex effect) we randomly shuffled subjects between male and female groups and recomputed the NMI between the permuted groups across all four levels of PACE-derived modularity. This shuffling procedure was repeated 10,000 times and the re-sampled NMI values were recorded.

By ranking our observed NMI among the re-sampled 10,000 NMI values, we detected significant sex differences in modularity starting at the first-level (P values: $<1e-04$, $1e-04$, $1.4e-03$ and $8.5e-03$ for hierarchical level 1 to 4 respectively; a combined P value would thus be in the scale of 10^{-14}). By contrast, a similar strategy to detect sex effect using any of the Q-based methods

failed to identify significant differences in the two sex-specific modular structures.

Figure 4 visualizes the PACE-identified modular structure sex differences (highlighted using blue arrows and rectangles) in HCP.

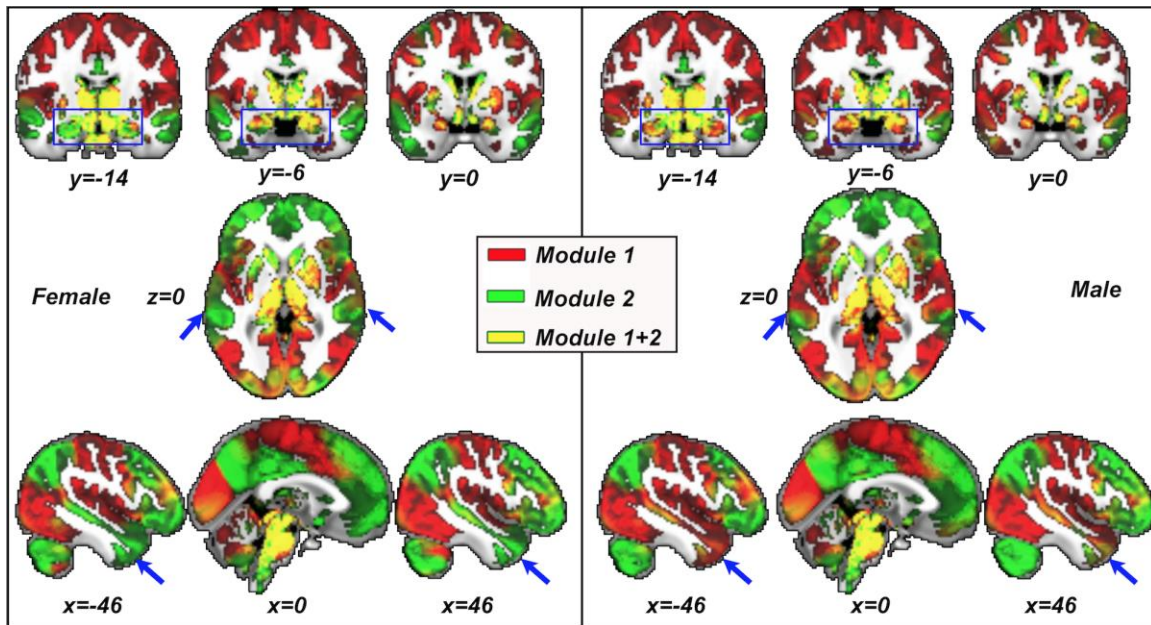


Figure 4. Visualization of PACE-identified sex-specific resting-state network modularity in females (left) and males (right) from the HCP dataset. Using permutation testing, sex-specific modularity differences are confirmed to be statistically significant throughout the entire PACE modular hierarchy starting at the first level. Here the results are visualized at first-level PACE, yielding two modules coded in red (module 1) and green (module 2). As HCP utilizes an ICA-based parcellation, modules thus overlap, in this case resulting in some regions colored in yellow.

Figure 4 shows sex differences in the bilateral temporal lobes, which was not detected using Q. These differences extended to the hippocampus and amygdala, which in females, were part of the green module, and in males formed part of the red module (although some of the right hemisphere inferior temporal pole was in the green module for males, see discussion section).

Discussion

In this study we proposed PACE, a new way of understanding how anti-correlations help define modularity of the resting-state fMRI connectome. The benefit function to be optimized exploits the intuition that a higher probability of an edge being anti-correlated indicates a higher probability of it connecting regions in different modules. Importantly, PACE permits a symmetric equivalent dual form, such that it can be equally conceived as placing edges that are most consistently positive within modules. Thus, PACE is intrinsically symmetrized.

Conventional Q-modularity based methods take a variable approach at negative edges. For example, many studies to date simply ignore anti-correlations by setting any values below a threshold (usually positive) to be zero (Sporns & Betzel, 2016), while others have proposed to down-weight negative edges in a somewhat heuristic fashion. The PACE method offers a novel and improved interpretation of left-tail fMRI networks, as traditionally, the left-tail network, i.e., those formed by negative edges alone, has been ignored as they are considered to be weak correlations that may “compromise” network attributes. For example, Schwarz and McGonigle (2011) argued that the left tail networks may not be biologically meaningful, despite noting that some connections were consistently observed in the negative-most tail networks, both with and without global signal removal. These tended to be long-range links, such as edges between the supramarginal gyrus and both the frontal medial orbital cortex and the posterior cingulate cortex. Schwarz and McGonigle thus recommended a “soft thresholding” approach be taken by replacing the hard

thresholding or binarization operation with a continuous mapping of all correlation values to edge weights, suppressing rather than removing weaker connections and avoiding issues related to network fragmentation.

Rather than taking an approach that interprets the magnitude of correlations as the strength of connectivity, PACE determines the probability of a correlation being positive or negative. While this is the most intuitive way to aggregate over the subjects, one could alternatively use, e.g., the average correlations over subjects. This second approach would, however, compromise the duality of PACE, and such a metric would be severely biased in the presence of outliers. Interestingly, PACE can also be thought of as a different way of binarizing, with a “two-way” thresholding at zero. Although thresholding at a different value is possible, it would compromise the equivalence of the PACE dual forms. Indeed, one could theoretically generalize PACE by setting $P^{\alpha\pm}_{i,j}$ to compute the probability of $e_{i,j}$ being larger or smaller than an arbitrary threshold alpha. However, in the case of a positive alpha, the left tail is no longer strictly anti-correlations.

To validate PACE, we used full rather than partial correlations. We chose this method because recent literature has suggested that in general, partial correlation matrices need to be very sparse (Peng, Wang, Zhou, & Zhu, 2009), and partial correlations have a tendency to reduce more connections than necessary. In dense networks such as fMRI-based brain networks, partial correlations have not been shown to be necessarily better than the Person correlation. Thus, partial correlations are often used in small networks that a)

have small numbers of connections or b) have been forced to be sparse by introducing a sparse penalty during whole-brain network generation (Lee, Lee, Kang, Kim, & Chung, 2011).

Following current practice in the literature, we compared PACE to computations of Q-based modular structures in both the HCP and F1000 datasets using the default setting in the BCT toolbox (the Louvain method). This produced substantially variable modular structure, not only across different Q-based formulations (right tail, left tail, absolute value, and symmetric and asymmetric combined), but also across multiple runs within each formulation. This raises questions about validity in interpreting Q-based modular results, and adds to another layer of confounds.

A secondary analysis further applied PACE to the investigation of potential sex differences in the resting functional connectome in the HCP dataset. Note, while sex differences have been reported in the structural connectome of the human brain (e.g. Szalkai, Varga, & Grolmusz, 2015), few studies have examined sex differences in the functional connectome in healthy individuals, and no studies to our knowledge have examined sex differences in higher-level connectome properties such as network modularity. Previously, one large study (Biswal et al., 2010) examined the functional connectome of the F1000 dataset using three methods: seed-based connectivity, independent component analysis (ICA) and frequency domain analyses. Across the three analytic methods, they found consistent effects of sex, with evidence of greater connectivity in males

than females in the temporal lobes, more so in the right hemisphere, and particularly when using ICA.

Our study revealed higher-level sex-specific connectome modularity differences in the temporal lobes, including the middle temporal gyrus, amygdala and hippocampus. The amygdala (Cahill, 2010) and hippocampus (Addis, Moscovitch, Crawley, & McAndrews, 2004) are important for emotional and autobiographic memory. Behavioural studies have reported sex differences in autobiographic memory retrieval (Seidlitz & Diener, 1998), particularly autobiographic memories associated with emotions (Davis, 1999), although not all studies have found behavioural differences (e.g. Compere et al., 2016). Sex differences in hippocampal and amygdala activity during autobiographic memory retrieval have also been reported (St. Jacques, Conway, & Cabeza, 2011; Young, Bellgowan, Bodurka, & Drevets, 2013). Researchers reporting sex differences in fMRI activity in studies such as these have argued that these findings are likely to reflect differential, sex-specific cognitive strategies for autobiographic memory retrieval (Compere et al., 2016; Seidlitz & Diener, 1998; Young et al., 2013). Our first-level PACE finding that in females, the amygdala and hippocampus are within the module that also contains the default mode network, whereas in males its located in the module largely consisting of the visual and somatomotor networks, is consistent with this proposal. It is also consistent with Damoiseaux et al (2016) who found that females had greater connectivity between the hippocampus and medial PFC than males, and Kogler et al (2016) who found that females had greater connectivity between the left

amygdala and left middle temporal gyrus than males. These medial prefrontal and lateral temporal regions form part of the brains default mode network (Fox et al., 2005). Thus together, these recent and preliminary findings may reflect stronger coupling within the default mode network and between the amygdala and the default mode network in females than in males, which would be consistent with previous reports of greater regional homogeneity (i.e. local connectivity, or synchrony of resting state activity in neighbouring voxels) in the right hippocampus and amygdala in females than males (Lopez-Larson, Anderson, Ferguson, & Yurgelun-Todd, 2011).

Limitations and future directions

With the PACE benefit function cast as a difference between inter-modular versus intra-modular mean edge negativity, the optimization problem is NP-hard and thus the global solution is not computable in realistic terms, especially when the number of modules is also an unknown variable to be estimated. Thus, we instead used a top-down hierarchical bifurcating solver that was previously extensively tested in PLACE, yielding modularity whose number of communities are restricted to powers of two (i.e. 2, 4, 8 etc.). Despite (or thanks to) this limitation, we showed that PACE results were robust and insensitive to multiple runs while recovering known resting-state networks. Although the novel PACE-based symmetrized functional modularity is shown to be a powerful and mathematically elegant approach to understanding anti-correlations in fMRI connectomes, it cannot be computed without robust estimates of frequencies.

Thus, here we tested PACE using large-N cohorts of HCP and 1000 functional connectomes. Although theoretically feasible, individual-level PACE would require multiple runs for each individual or alternative ways of estimating these frequencies, and it is unclear how one extends to dynamic connectomes. Nevertheless, testing specific effects can be achieved with careful permutation testing while controlling for other variables (such as age), as we demonstrated in our secondary analyses showing significant sex effects in the temporal lobes. Future research could investigate whether our findings of sex differences in functional connectivity are supported by structural evidence, such as via analysis of DTI connectomes, to replicate this finding of increased DMN-temporal lobe connectivity in females compared to males. Network neuroscience is a rapidly emerging field, and recently, a novel study has utilized the rich dataset provided by the HCP to develop a new multimodal method for parcellating the human cerebral cortex into 180 areas per hemisphere (Glasser et al., 2016). This semi-automated method incorporates machine-learning classification to detect cortical areas. It would be interesting to apply PACE to this new parcellation once the classifier becomes publically available.

Conclusions

This methodological report illustrates the problem that existing Q-based methods of defining modularity return variable results. In contrast, the novel PACE framework provided here returns consistent and reproducible modularity. When applied to the HCP dataset, we showed that our new method yielded

similar results compared to existing methods, providing evidence for convergent validity. Furthermore, given the high reliability of this new method, we have been able to demonstrate sex differences in resting state connectivity that are not detected with traditional methods. Future research using PACE is encouraged to further demonstrate the superiority of this approach to defining brain modularity in disease populations. (the PACE MATLAB code will be online and publicly available once this paper is accepted).

References

- Addis, D. R., Moscovitch, M., Crawley, A. P., & McAndrews, M. P. (2004). Recollective qualities modulate hippocampal activation during autobiographical memory retrieval. *Hippocampus*, *14*(6), 752-762. doi:10.1002/hipo.10215
- Ajilore, O., Zhan, L., GadElkarim, J. J., Zhang, A. F., Feusner, J., Yang, S. L., . . . Leow, A. D. (2013). Multimodal brain connectivity analysis using functional-by-structural hierarchical mapping. *Neuropsychopharmacology*, *38*, S163-S163.
- Alexander-Bloch, A., Lambiotte, R., Roberts, B., Giedd, J., Gogtay, N., & Bullmore, E. T. (2012). The discovery of population differences in network community structure: New methods and applications to brain functional networks in schizophrenia. *Neuroimage*, *59*(4), 3889-3900. doi:10.1016/j.neuroimage.2011.11.035
- Aynaud, T., Blondel, V. D., Guillaume, J. L., & Lambiotte, R. (2013). Multilevel local optimization of modularity. In C.-E. Bichot & P. Siarry (Eds.), *Graph Partitioning*. Hoboken, NJ: John Wiley & Sons, Inc.
- Beckmann, C. F., DeLuca, M., Devlin, J. T., & Smith, S. M. (2005). Investigations into resting-state connectivity using independent component analysis. *Philosophical Transactions of the Royal Society B-Biological Sciences*, *360*(1457), 1001-1013. doi:10.1098/rstb.2005.1634
- Betzal, R. F., Fukushima, M., He, Y., Zuo, X. N., & Sporns, O. (2016). Dynamic fluctuations coincide with periods of high and low modularity in resting-state functional brain networks. *Neuroimage*, *127*, 287-297. doi:10.1016/j.neuroimage.2015.12.001
- Biswal, B. B., Mennes, M., Zuo, X. N., Gohel, S., Kelly, C., Smith, S. M., . . . Milham, M. P. (2010). Toward discovery science of human brain function. *Proceedings of the National Academy of Sciences of the United States of America*, *107*(10), 4734-4739. doi:10.1073/pnas.0911855107
- Blondel, V. D., Guillaume, J. L., Lambiotte, R., & Lefebvre, E. (2008). Fast unfolding of communities in large networks. *Journal of Statistical Mechanics-Theory and Experiment*, *12*. doi:10.1088/1742-5468/2008/10/p10008
- Brown, J., Rudie, J. D., Bandrowski, A., Van Horn, J. D., & Bookheimer, S. Y. (2012). The UCLA multimodal connectivity database: A web-based platform for brain connectivity matrix sharing and analysis. *Frontiers in Neuroinformatics*, *6*, 17. doi:10.3389/fninf.2012.00028
- Bullmore, E. T., & Sporns, O. (2009). Complex brain networks: Graph theoretical analysis of structural and functional systems. *Nature Reviews Neuroscience*, *10*(3), 186-198. doi:10.1038/nrn2575
- Butts, C. T. (2003). Network inference, error, and informant (in)accuracy: A Bayesian approach. *Social Networks*, *25*(2), 103-140. doi:10.1016/s0378-8733(02)00038-2
- Cahill, L. (2010). Sex influences on brain and emotional memory: The burden of proof has shifted. In I. Savic (Ed.), *Sex Differences in the Human Brain, Their Underpinnings and Implications* (Vol. 186, pp. 29-40). Amsterdam: Elsevier Science Bv.

- Compere, L., Sperduti, M., Gallarda, T., Anssens, A., Lion, S., Delhommeau, M., . . . Piolino, P. (2016). Sex differences in the neural correlates of specific and general autobiographical memory. *Frontiers in Human Neuroscience, 10*, 16. doi:10.3389/fnhum.2016.00285
- Danon, L., Diaz-Guilera, A., Duch, J., & Arenas, A. (2005). Comparing community structure identification. *Journal of Statistical Mechanics-Theory and Experiment, 10*. doi:10.1088/1742-5468/2005/09/p09008
- Davis, P. J. (1999). Gender differences in autobiographical memory for childhood emotional experiences. *Journal of Personality and Social Psychology, 76*(3), 498-510. doi:10.1037/0022-3514.76.3.498
- Dijkstra, E. W. (1959). A note on two problems in connexion with graphs. *Numerische Mathematik, 1*(1), 269-271.
- Fornito, A., Zalesky, A., & Breakspear, M. (2013). Graph analysis of the human connectome: Promise, progress, and pitfalls. *Neuroimage, 80*, 426-444. doi:10.1016/j.neuroimage.2013.04.087
- Fortunato, S., & Barthelemy, M. (2007). Resolution limit in community detection. *Proceedings of the National Academy of Sciences of the United States of America, 104*(1), 36-41. doi:10.1073/pnas.0605965104
- Fox, M. D., Snyder, A. Z., Vincent, J. L., Corbetta, M., Van Essen, D. C., & Raichle, M. E. (2005). The human brain is intrinsically organized into dynamic, anticorrelated functional networks. *Proceedings of the National Academy of Sciences of the United States of America, 102*(27), 9673-9678. doi:10.1073/pnas.0504136102
- GadElkarim, J. J., Ajilore, O., Schonfeld, D., Zhan, L., Thompson, P. M., Feusner, J. D., . . . Leow, A. D. (2014). Investigating brain community structure abnormalities in bipolar disorder using path length associated community estimation. *Human Brain Mapping, 35*(5), 2253-2264. doi:10.1002/hbm.22324
- GadElkarim, J. J., Schonfeld, D., Ajilore, O., Zhan, L., Zhang, A. F., Feusner, J. D., . . . Leow, A. D. (2012). A framework for quantifying node-level community structure group differences in brain connectivity networks. *Medical image computing and computer-assisted intervention : MICCAI ... International Conference on Medical Image Computing and Computer-Assisted Intervention, 15*(Pt 2), 196-203.
- Glasser, M. F., Coalson, T. S., Robinson, E. C., Hacker, C. D., Harwell, J., Yacoub, E., . . . Van Essen, D. C. (2016). A multi-modal parcellation of human cerebral cortex. *Nature, 1*-8.
- Guimera, R., & Amaral, L. A. N. (2005). Functional cartography of complex metabolic networks. *Nature, 433*(7028), 895-900. doi:10.1038/nature03288
- Guimera, R., & Sales-Pardo, M. (2009). Missing and spurious interactions and the reconstruction of complex networks. *Proceedings of the National Academy of Sciences of the United States of America, 106*(52), 22073-22078. doi:10.1073/pnas.0908366106
- Guimera, R., Sales-Pardo, M., & Amaral, L. A. N. (2004). Modularity from fluctuations in random graphs and complex networks. *Physical Review E, 70*(2), 4. doi:10.1103/PhysRevE.70.025101

- Lamar, M., Ajilore, O., Leow, A., Charlton, R., Cohen, J., GadElkarim, J., . . . Kumar, A. (2016). Cognitive and connectome properties detectable through individual differences in graphomotor organization. *Neuropsychologia*, *85*, 301-309. doi:10.1016/j.neuropsychologia.2016.03.034
- Lancichinetti, A., & Fortunato, S. (2009). Community detection algorithms: A comparative analysis. *Physical Review E*, *80*(5), 11. doi:10.1103/PhysRevE.80.056117
- Lee, H., Lee, D. S., Kang, H., Kim, B. N., & Chung, M. K. (2011). Sparse brain network recovery under compressed sensing. *Ieee Transactions on Medical Imaging*, *30*(5), 1154-1165. doi:10.1109/tmi.2011.2140380
- Lopez-Larson, M. P., Anderson, J. S., Ferguson, M. A., & Yurgelun-Todd, D. (2011). Local brain connectivity and associations with gender and age. *Developmental Cognitive Neuroscience*, *1*(2), 187-197. doi:10.1016/j.dcn.2010.10.001
- Meunier, D., Lambiotte, R., & Bullmore, E. T. (2010). Modular and hierarchically modular organization of brain networks. *Frontiers in neuroscience*, *4*, 200. doi:10.3389/fnins.2010.00200
- Newman, M. E. J. (2006). Modularity and community structure in networks. *Proceedings of the National Academy of Sciences of the United States of America*, *103*(23), 8577-8582. doi:10.1073/pnas.0601602103
- Newman, M. E. J., & Girvan, M. (2004). Finding and evaluating community structure in networks. *Physical Review E*, *69*(2), 15. doi:10.1103/PhysRevE.69.026113
- Peng, J., Wang, P., Zhou, N. F., & Zhu, J. (2009). Partial correlation estimation by joint sparse regression models. *Journal of the American Statistical Association*, *104*(486), 735-746. doi:10.1198/jasa.2009.0126
- Reichardt, J., & Bornholdt, S. (2006). Statistical mechanics of community detection. *Physical Review E*, *74*(1), 14. doi:10.1103/PhysRevE.74.016110
- Ronhovde, P., & Nussinov, Z. (2009). Multiresolution community detection for megascale networks by information-based replica correlations. *Physical Review E*, *80*(1), 18. doi:10.1103/PhysRevE.80.016109
- Rubinov, M., & Sporns, O. (2010). Complex network measures of brain connectivity: Uses and interpretations. *Neuroimage*, *52*(3), 1059-1069. doi:10.1016/j.neuroimage.2009.10.003
- Rubinov, M., & Sporns, O. (2011). Weight-conserving characterization of complex functional brain networks. *Neuroimage*, *56*(4), 2068-2079. doi:10.1016/j.neuroimage.2011.03.069
- Schwarz, A. J., & McGonigle, J. (2011). Negative edges and soft thresholding in complex network analysis of resting state functional connectivity data. *Neuroimage*, *55*(3), 1132-1146. doi:10.1016/j.neuroimage.2010.12.047
- Seidnitz, L., & Diener, E. (1998). Sex differences in the recall of affective experiences. *Journal of Personality and Social Psychology*, *74*(1), 262-271. doi:10.1037//0022-3514.74.1.262
- Simon, H. A. (2002). Near decomposability and the speed of evolution. *Industrial and Corporate Change*, *11*(3), 587-599. doi:10.1093/icc/11.3.587

- Sporns, O., & Betzel, R. F. (2016). Modular brain networks. In S. T. Fiske (Ed.), *Annual Review of Psychology, Vol 67* (Vol. 67, pp. 613-640). Palo Alto: Annual Reviews.
- St. Jacques, P. L., Conway, M. A., & Cabeza, R. (2011). Gender differences in autobiographical memory for everyday events: Retrieval elicited by SenseCam images versus verbal cues. *Memory, 19*(7), 723-732.
doi:10.1080/09658211.2010.516266
- Sun, Y., Danila, B., Jovic, K., & Bassler, K. E. (2009). Improved community structure detection using a modified fine-tuning strategy. *Epl, 86*(2), 6.
doi:10.1209/0295-5075/86/28004
- Szalkai, B., Varga, B., & Grolmusz, V. (2015). Graph theoretical analysis reveals: Women's brains are better connected than men's. *Plos One, 10*(7), 30.
doi:10.1371/journal.pone.0130045
- Van Essen, D. C., Smith, S. M., Barch, D. M., Behrens, T. E. J., Yacoub, E., Ugurbil, K., & Consortium, W. U.-M. H. (2013). The WU-Minn Human Connectome Project: An overview. *Neuroimage, 80*, 62-79. doi:10.1016/j.neuroimage.2013.05.041
- Van Essen, D. C., Ugurbil, K., Auerbach, E., Barch, D., Behrens, T. E. J., Bucholz, R., . . . Wu-Minn, H. C. P. C. (2012). The Human Connectome Project: A data acquisition perspective. *Neuroimage, 62*(4), 2222-2231.
doi:10.1016/j.neuroimage.2012.02.018
- Ye, A. Q., Zhan, L., Conrin, S., GadElKarim, J., Zhang, A. F., Yang, S. L., . . . Leow, A. (2015). Measuring embeddedness: Hierarchical scale-dependent information exchange efficiency of the human brain connectome. *Human Brain Mapping, 36*(9), 3653-3665. doi:10.1002/hbm.22869
- Young, K. D., Bellgowan, P. S. F., Bodurka, J., & Drevets, W. C. (2013). Functional neuroimaging of sex differences in autobiographical memory recall. *Human Brain Mapping, 34*(12), 3320-3332. doi:10.1002/hbm.22144
- Zhang, A., Leow, A., Zhan, L., GadElKarim, J., Moody, T., Khalsa, S., . . . Feusner, J. (2016). Brain connectome modularity in weight-restored anorexia nervosa and body dysmorphic disorder. *Psychological Medicine, 1*-13.